MOLECULAR AND CELLULAR BIOLOGY, Dec. 1990, p. 6755–6758
0270-7306/90/126755-04$02.00/0

Vol. 10, No. 12

NOTES

Germ Line Transmission of an Inactive N-*myc* Allele Generated by Homologous Recombination in Mouse Embryonic Stem Cells

BRIAN R. STANTON, SUSAN W. REID, AND LUIS F. PARADA*

Molecular Embryology Group, ABL-Basic Research Program, NCI-Frederick Cancer Research and Development Center, P.O. Box B, Frederick, Maryland 21702-1201

Received 4 June 1990/Accepted 24 August 1990

We have disrupted one allele of the N-*myc* locus in mouse embryonic stem (ES) cells by using homologous recombination techniques and have obtained germ line transmission of null N-*myc* ES cell lines with transmission of the null N-*myc* allele to the offspring. The creation of mice with a deficient N-*myc* allele will allow the generation of offspring bearing null N-*myc* alleles in both chromosomes and permit study of the role that this proto-oncogene plays in embryonic development.

The N-*myc* gene was first identified as an amplified sequence in human neuroblastoma cell lines and tumors (8, 9, 13). These are pediatric tumors of embryonal origin that arise in the peripheral nervous system (commonly the adrenal medulla). N-*myc* gene expression is detected predominantly in the mouse embryo (10, 16; L. F. Parada and D. Sassoon, submitted for publication) as well as in embryonic stem (ES) cell lines (7; this report). Studies undertaken to further investigate N-*myc* expression during embryonic development have generated evidence that transcription of this gene is confined to specific cell types, and it is thought that N-*myc* plays a formative role in embryonic development (5; Parada and Sassoon, submitted).

With the aim of creating an experimental system that will allow direct study of N-*myc* function and regulation, we have undertaken a reverse genetic approach, exploiting ES cells (1, 11, 12, 14) to mutagenize an allele of the N-*myc* gene and to transmit it into the germ line of mice. The principle of site-directed mutagenesis in ES cells is based on the ability to select and distinguish cells that have integrated transfected DNA by homologous versus nonhomologous recombination. Early studies (4, 15) indicated that recipient cells integrate exogenous DNA via mechanisms of homologous recombination at an efficiency of approximately 10^{-3}. More recent information suggests that the frequency of homologous recombination is highly variable and may depend on such parameters as sequence, chromosomal location, and the transcriptional state of the gene under study (Allan Bradley, personal communication). Therefore, the exact nature of the selection strategy devised to detect homologous recombination events is of primary importance.

To test for N-*myc* expression, poly(A)$^+$ RNA was isolated from D3 ES cells and submitted to Northern (RNA) analysis. A 2.9-kb N-*myc* transcript was detected in D3 cells, indicating that the endogenous N-*myc* gene was transcribed in these cells (Fig. 1). A 5.5-kbp fragment of genomic N-*myc* sequences lacking any known endogenous promoter element (Fig. 2) was used as the framework for the recombination cassette. By use of synthetic adapters, a fusion of the first 19 N-*myc* codons to the *neo* gene coding sequences was prepared and designated pNMYC*neo*F (Fig. 2). Upon introduction of pNMYC*neo*F into cells, transcription of the *neo* gene

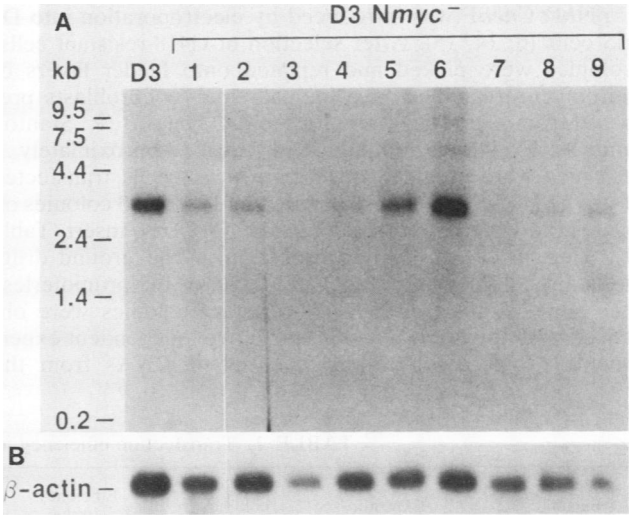

FIG. 1. (A) Northern transfer analysis of RNA isolated from parental and recombinant ES cell lines, using the N-*myc* *Bam*HI-*Cla*I fragment described in Fig. 2 as a probe. Lanes: D3, Parental D3 ES cell line; D3 N*myc*$^-$ 1 to 9, nine independent cell clones bearing a *neo* insert at one of the N-*myc* alleles. Migration of molecular size standards is indicated at the left. (B) Rehybridization of the same filter with a mouse β-actin probe to assess relative amounts of RNA present in each lane. Poly(A)$^+$ RNA (1 to 2 μg) was separated on 1.1% formaldehyde–1.2% agarose gels and transferred to nylon membranes (Zetabind; CUNO). Hybridization was performed by using random-primed probes in 250 mM sodium phosphate (pH 7.2)–1 mM EDTA–7% sodium dodecyl sulfate (SDS)–1% bovine serum albumin. Filters were washed twice for 30 min at 65°C in 40 mM sodium phosphate (pH 7.2)–5% SDS–0.5% bovine serum albumin, followed by two washes in 40 mM sodium phosphate (pH 7.2)–1% SDS. Densitometry scan comparison of the N-*myc*$^-$ lanes versus the D3/β-actin lane display ratios from 0.3 to 0.5, as anticipated. Two exceptions, lanes 5 (1.1) and 6 (2.1), were observed. These deviants may represent deregulation of the functional allele.

* Corresponding author.

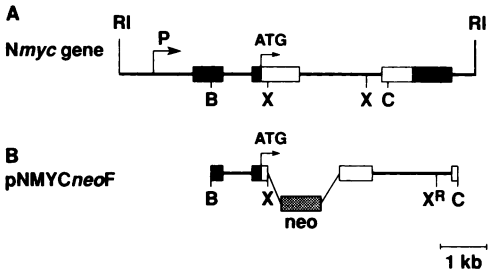

FIG. 2. Schematic diagram of the N-*myc* recombination cassette. (A) The N-*myc* locus contained within pN7.7 (3). The *Bam*HI-*Cla*I fragment of pN7.7 was used as the framework for the recombination cassette (B). The *Xho*I site located upstream of exon 3 was filled in with Klenow enzyme (X^R), and an 850-bp *Eag*I-*Sal*I *neo* fragment was inserted into the remaining *Xho*I site located 57 nucleotides downstream of the N-*myc* initiator ATG through the use of a synthetic oligonucleotide. Symbols: ■, noncoding exons; □, coding portions of exons; ▩, the bacterial *neo* gene. P, Approximate region of the promoter; ATG, the initiation codon for N-*myc*. Restriction sites: RI, *Eco*RI; B, *Bam*HI; X, *Xho*I; C, *Cla*I.

would depend on the functionality of the resultant N-*myc*–*neo* hybrid protein and on integration adjacent to a transcriptionally active promoter. This latter requirement should allow discrimination against nonhomologous integration into the genome and enrich for the desired homologous recombination event downstream of the endogenous N-*myc* promoter.

pNMYC*neo*F was introduced by electroporation into D3 ES cells (6, 14, 15). After selection of G418-resistant cells, colonies were picked and replated onto feeder layers of mitomycin-treated primary mouse embryo fibroblasts prepared from mice transgenic for the *neo* gene (B. R. Stanton and L. F. Parada, unpublished data). Approximately 5 colonies were obtained on each plate of cells transfected with the N-*myc*–*neo* construct, versus 100 to 500 colonies on plates transfected with the control of pMC1*neo* insert (Table 1). Thus, a 20- to 100-fold reduction in background drug-resistant colonies was achieved by use of the promoterless *neo* gene. A total of 99 G418-resistant colonies were obtained with the N-*myc*–*neo* insert in five independent experiments (Table 1). Southern analysis of DNAs from the

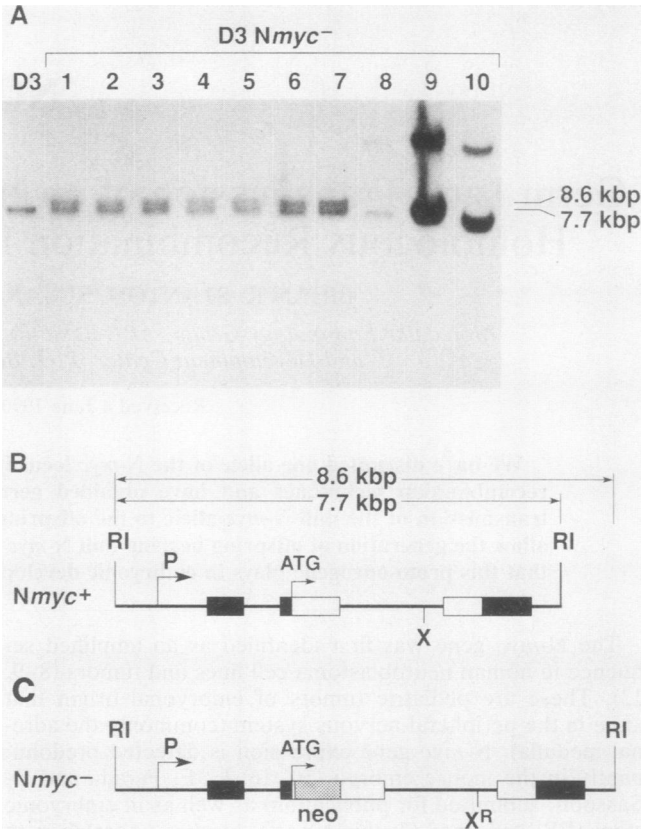

FIG. 3. Structural analysis at the N-*myc* locus of homologous recombinant cell clones and schematic representation of the N-*myc* locus after inactivation by homologous recombination. (A) Southern analysis of the N-*myc* locus in parental D3 cells and in 10 independently derived G418-resistant, homologous recombinant cell lines (lanes D3 N*myc*⁻ 1 to 10). The sizes of the predicted 7.7- and 8.6-kbp *Eco*RI fragments are indicated on the right. (B) Normal N-*myc* locus contained within a 7.7-kbp *Eco*RI fragment. (C) The null N-*myc* allele enlarged by 0.9 kbp as a result of the inclusion of the *neo* gene. Symbols are as for Fig. 2.

TABLE 1. Transfection efficiency and frequency of homologous recombination

Plasmid	Expt no.	No. of colonies obtained[a]	Efficiency (10^{-6})[b]	Ratio, pMC1*neo*/ pNMYC*neo*F	No. of colonies screened	No. of recombinants	Frequency (%)
pMC1*neo*	1	382	38.2	–	–	–	–
	2	124	12.4	–	–	–	–
	3	>400	>40.0[c]	–	–	–	–
	4	>400	>40.0[c]	–	–	–	–
	5	>400	>40.0[c]	–	–	–	–
pNMYC*neo*F	1	9	0.9	42.4	9	2 (1)[d]	33
	2	22	2.2	5.6	5	1	20
	3	21	2.1	>19.0[c]	21	1 (2)[d]	14
	4	27	2.7	>14.0[c]	27	2	7
	5	20	2.0	>20.0[c]	20	1	5

[a] Cells were scored at the end of the experiment, as indicated by the absence of colonies on negative control plates. Positive controls (i.e., pMC1*neo*) were stained with methylene blue and counted. Plates containing more than 400 colonies were not counted and are designated >400.

[b] Calculated by dividing the number of colonies obtained by the number of cells electroporated. A total of 10^7 cells were used in all experiments, and approximately 50% of the cells survived electoporation.

[c] Based on a value of 400 colonies on the control plates; therefore, the value given is the minimum estimate.

[d] Number in parentheses indicates homologous recombinants that have integrated more than one copy of the recombination cassette into the N-*myc* locus and result in disruption of the gene.

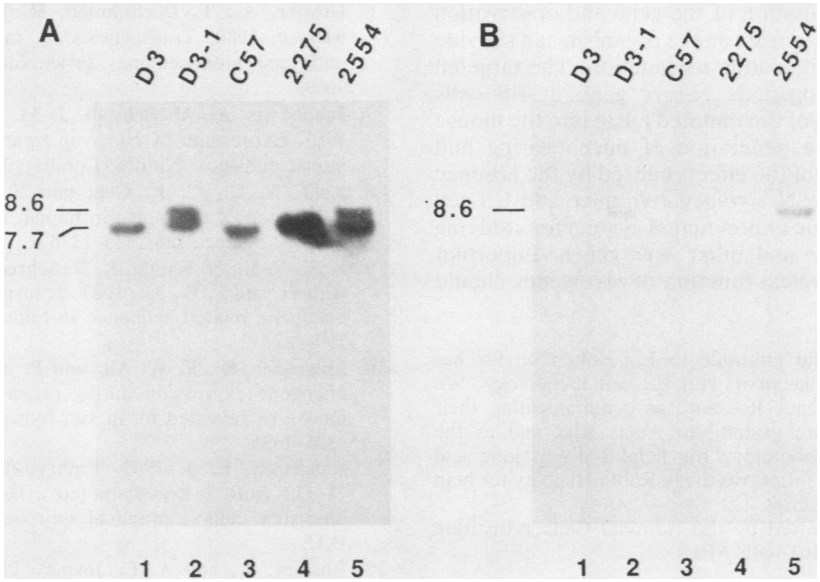

FIG. 4. Southern blot analysis demonstrating the presence of the disrupted N-*myc* allele in A^W progeny of a chimeric mouse. (A) *Eco*RI-digested genomic DNA hybridized with an N-*myc* probe. Lanes: 1, D3 ES cell line; 2, null N-*myc* D3-1 cell line; 3, tail DNA from recipient (57BL mouse strain; 4, tail DNA from parental chimera 2275; 5, tail DNA from agouti offspring 2554. (B) Same order as in panel A, but the probe in this case was *neo*. The indicated size markers are in kilobase pairs.

drug-resistant clones was then performed to determine the nature of the insertion. A homologous recombination event results in the diagnostic increase in size of the endogenous 7.7-kbp *Eco*RI N-*myc*-hybridizing fragment to 8.6 kbp, caused by the insertion of the *neo* fragment. The Southern blot shown in Fig. 3 indicates the presence of the novel 8.6-kbp band when hybridized with an N-*myc* or a *neo* probe.

The results of our studies to date are summarized in Table 1. Ten cell lines having one damaged N-*myc* allele have been obtained. Seven lines integrated the DNA by homologous recombination involving simple replacement of the endogenous N-*myc* sequences, while three cell lines have a more complex integration pattern apparently resulting from insertion of two complete tandem copies interrupted by a variably deleted third copy (Fig. 3, lanes 8 to 10). Expression of the remaining functional N-*myc* allele in the recombinant cell lines was examined by Northern analysis (Fig. 1). Seven of nine cell lines analyzed displayed a stoichiometric reduction of N-*myc* expression, as determined by a comparative densitometry scan normalized by the signal obtained with a mouse β-actin probe hybridized to the same filter (not shown).

During construction of the recombination cassette, an *Xho*I restriction site present in the genomic sequence was removed. This polymorphism (X^R) is located 233 bp from the 3′ end of the recombination cassette (Fig. 2). Southern analysis of DNA digested with *Xho*I has revealed the presence of the functional *Xho*I site in all of the simple recombinant cell lines isolated so far. The lack of parity for the polymorphism may be explained by various alternatives. Either (i) the introduced linear recombination cassette is degraded before its participation in recombination, thus removing the X^R site, (ii) the downstream (3′-end) crossover occurred exclusively on the 5′ side of the X^R site, or (iii) the polymorphism was included in the recombination event but the subsequent repair process was unidirectional, always using the endogenous strand as the template.

Blastocyst injections were performed with two of the 10 null N-*myc* ES cell lines (D3-1 and D3-9). Four of the D3-1 recipient C57BL male chimeras have given rise to agouti (A^W) offspring. Chimera 2275 and its offspring have been analyzed in detail. An A^W male pup (no. 2554) was born in the fourth litter, two A^W male offspring were born in the fifth litter, and several more have been produced in subsequent litters. Evidently, this chimera contains a mosaic germ line with partial ES cell contribution. The D3 contribution to the offspring was first determined by their A^W coat color and by the presence of the D3-derived *Gpi-1*^{a} (glucose phosphate isomerase, *a* allele) isoform in the chimera. Tail genomic DNA Southern blots have verified the presence of the recombined N-*myc* allele, including the *neo* gene, in progeny 2254 (Fig. 4). Thus, the novel 8.6-kbp *Eco*RI fragment seen in the D3 null N-*myc* cells is present in the male offspring. This fragment also hybridized with a *neo* probe (Fig. 4). The genotype at the N-*myc* locus of additional D3-1- derived agouti offspring has been determined, and additional independent N-*myc*-negative mice of both sexes have been obtained. No overt phenotypic changes have been observed in the heterozygotic mice.

While this report was in preparation, Charron et al. reported the targeted mutagenesis of N-*myc* in ES cells but did not obtain germ line transmission (2). Here we show that the N-*myc*–*neo* hybrid protein is functional, and this hybrid gene approach may be a generally applicable tool for future studies of this nature. We note that there has been a second disrupted N-*myc* allele transmitted into the germ line of mice (C. Moens, A. Joyner, and J. Rossant, personal communication) by using a construct similar to that of Charron and co-workers (personal communication).

Classical genetic analysis takes advantage of spontaneous or experimentally derived mutants to gain insight into the functions of genes. These approaches occur at the organism level without a priori knowledge of the molecular foundation of an observed phenotype. Reverse genetics is based on the opposite approach, in which a gene is identified but the

function is unknown. Mutation of the gene and observation of the phenotypic consequences on the organism can provide a powerful means for elucidating its function. The targeted mutagenesis of an endogenous N-*myc* gene in ES cells followed by introduction of the mutated allele into the mouse germ line will allow the generation of mice bearing null N-*myc* alleles and study of the effects caused by the absence of this gene in vivo. The N-*myc*-negative mice and ES cell lines also provide a unique experimental system for studying the regulation of N-*myc* and other *myc* genes. Important clues about the physiological function of *myc* genes should also emerge.

We express our profound gratitude to Liz Robertson for her continual help and encouragement with ES cell technology. We thank Alex Joyner and Janet Rossant for communicating their unpublished results and are grateful to Amar Klar and to the members of the Parada laboratory for helpful discussions and critical reading of the manuscript; we thank Robin Handley for help in preparation of the manuscript.

This research was supported by the National Cancer Institute under contract N01-CO-74101 with ABL.

LITERATURE CITED

1. **Capecchi, M. R.** 1989. Altering the genome by homologous recombination. Science **244**:1288–1292.
2. **Charron, J., B. A. Malynn, E. J. Robertson, S. P. Goff, and F. W. Alt.** 1990. High-frequency disruption of the N-*myc* gene in embryonic stem and pre-B cell lines by homologous recombination. Mol. Cell. Biol. **10**:1799-1804.
3. **DePinho, R. A., E. Legouy, L. B., Feldman, N. E. Kohl, G. D. Yancopoulos, and F. W. Alt.** 1986. Structure and expression of the murine N*myc* gene. Proc. Natl. Acad. Sci. USA **83**:1827–1831.
4. **Doetschman, T., R. G. Gregg, N. Maeda, M. L. Hooper, D. W. Melton, S. Thompson, and O. Smithies.** 1987. Targeted correction of a mutant HPRT gene in mouse embryonic stem cells. Nature (London) **330**:576–578.
5. **Downs, K. M., G. R. Martin, and J. M. Bishop.** 1989. Contrasting patterns of *myc* and N-*myc* expression during gastrulation of the mouse embryo. Genes Dev. **3**:860–869.
6. **Gossler, A., T. Doetschman, R. Korn, E. Serfling, and R. Kemler.** 1986. Transgenesis by means of blastocyst-derived embryonic stem cell lines. Proc. Natl. Acad. Sci. USA **83**:9065–9069.
7. **Jakobovits, A., M. Schwab, J. M. Bishop, and G. R. Martin.** 1985. Expression of N*myc* in teratocarcinoma stem cells and mouse embryos. Nature (London) **318**:188–191.
8. **Kohl, N. E., C. E. Gee, and F. W. Alt.** 1984. Activated expression of the N*myc* in human neuroblastomas and related tumors. Science **226**:1335–1336.
9. **Kohl, N. E., N. Kanda, R. R. Schreck, G. Bruns, S. A. Latt, F. Gilbert, and F. W. Alt.** 1983. Transposition and amplification of oncogene related sequence in human neuroblastoma. Cell **35**: 359–367.
10. **Mugrauer, G., F. W. Alt, and P. Ekbolm.** 1988. N*myc* proto-oncogene expression during organogenesis in the developing mouse as revealed by in situ hybridization. J. Cell Biol. **107**: 1325–1335.
11. **Robertson, E. J.** 1987. Embryo-derived stem cell lines, p. 71–112. *In* R. J. Robertson (ed.), Teratocarcinomas and embryonic stem cells: a practical approach. IRL Press, Washington, D.C.
12. **Rossant, J., and A. L. Joyner.** 1989. Towards a molecular-genetic analysis of mammalian development. Trends Genet. **5**:277–283.
13. **Schwab, M., K. Alitalo, K. H. Klempnauer, H. E. Varmus, J. M. Bishop, F. Gilbert, G. Brodeur, M. Goldstein, and J. Trent.** 1983. Amplified DNA with limited homology to *myc* cellular oncogene is shared by human neuroblastoma cell lines and a neuroblastoma tumor. Nature (London) **305**:245–248.
14. **Schwartzberg, P. L., S. P. Goff, and E. J. Robertson.** 1989. Germ-line transmission of a c-abl mutation produced by targeted gene disruption in ES cells. Science **246**:799–803.
15. **Thomas, K. R., and M. R. Capecchi.** 1987. Site-directed mutagenesis by gene targeting in mouse embryo-derived stem cells. Cell **51**:503–512.
16. **Zimmerman, K. A., G. D. Yancopoulos, R. G. Collum, R. K. Smith, N. E. Kohl, K. A. Denis, M. M. Nau, O. N. Witte, D. Toran-Allerand, C. E. Gee, et al.** 1986. Differential expression of *myc* family genes during murine development. Nature (London) **319**:780–783.